EPJ Web of Conferences **26**, 03005 (2012)
DOI: 10.1051/epjconf/20122603005

Development of new Hopkinson's device dedicated to rib's bone characterisation

O. Mayeur, G. Haugou, F. Chaâri, R. Delille, P. Drazetic, and E. Markiewicz

LAMIH UMR 8201 - CNRS, University of Valenciennes, 59313 Valenciennes Cedex 9, France

Abstract. This study presents an original approach for the design of adapted Hopkinson device dedicated to the characterisation of human ribs' cortical bone. The quasi-static study carried out on flat samples coming from this anatomical part highlighted the importance of the critical effect of sample shape and location on the accuracy of identify mechanical behaviour. The access to higher rates of strains, Hopkinson bars technique are classically required whatever compression or tension loadings. Classical designs of measurement bars are not suitable for this purpose due to the complexity of specimen's geometry (thickness variation). In this context, a new design of SHTB is studied here on the basis on a Finite Element approach of the set measurement bars/biological coupon. Finite Element simulations have been conducted using Abaqus explicit code by varying the design configuration. The comparison on input and output elastic waves suggests a set of small diameter bars in polyamide 66 for a better signal measurement.

1 Introduction

Thorax is one of the segments frequently involved in road accident. Despite that, FE models of the thorax are commonly simplified and don't take into account all rib's parameters. The FE model improvement is most difficult in this anatomical part because of the complex geometry of ribs and its internal structure composed by thin cortical thickness, spongy bone variability and narrow. Previous study has performed on ribs and on the whole ribcage, through experimental tests (Kuppa [1], Vezin [2]) or computing simulation (Robin [3], Song [4]). The ribs present a thin cortical thickness influencing the thorax response. This cortical bone is a non-homogenous material with voids and mechanical characterisation is needed on this constitutive part to access more biofidelic FE model. For a better assessment of injury criterion during crash simulations the numerical model of the thorax should be refined in term of accurate geometry and material properties. The European project THOMO tries to answer these goals by developing a numerical model of the human thorax and upper extremities, build from Post Mortem Human Subjects. Quasi-static tests are made in the frame of this project. These mechanical tests are performed on thin cortical bone sample of human ribs. In literature, tensile tests have been made on bovine bones (Ferreira [5], Wright [6]) but less often on human ribs. Only Subit [7] and Kemper [8] have worked on this challenging task through quasi-static and dynamic tensile tests. The authors managed the curvature of the specimen by taking the flattest rib section as possible and then sanding to remove defects and ensure that the gage length was flat. The dynamical tests are performed on hydraulic jack on dog-bone lamella of rib's cortical bone. Quasi-static tensile tests have been performed on THOMO project on the same sample shape. The aim of this study is to extend the quasi-static results to dynamic using Split-Hopkinson Tensile Bars device. At this sample size, classical designs of SHTB are not suitable due to the complexity of specimen's geometry (thickness sample). It was interesting to develop, thanks to FE models, new Hopkinson's device dedicated to rib's cortical bone characterisation.

2 Material and method

2.1 Samples harvesting

The mechanical characterisation is validated and applied on samples harvested on one THOMO subject. The subject was supplied to the project by the Body Donation program of the University of Paris with respect to ethical rules and a scientific committee approval. The tested subject, referenced S605 in the study, is a 73 year old male (61 kg weight to 171 cm height). The body was frozen in an upright position to fix the ribs, the spine, and the internal organs in an anatomical position close to live beings. Right ribs were taken from the thorax and delivered to the UVHC for the geometrical protocol and mechanical test. The choice of the sample location is related to the geometrical analysis of rib cortical bone thickness. Numerical model of entire ribs are generated thanks to μCT-scan reconstruction (Figure 1(b)) and the data are analysed to define the best coupon location.

This geometrical protocol is developed to eliminate extra-zones where no extraction can be ensured. Therefore the appropriated location (cortical bone thickness and curvature of rib) are selected for coupon machining. This analyse gives also information about the position on the rib to study the influence of sample location on mechanical behaviour.

The 2^{nd} to 10^{th} rib of the subject 605 was investigated in this study. Because of the limited thickness of cortical bone in the ribs, a special procedure was established to obtain precisely geometry controlled samples. This procedure employed surgical saw for debit step, polisher to rectify the flatness of cortical bone structure and then a dedicated μ milling device to finalize the sample shape. The first extraction provides a sandwich structure separated with a surgical saw. The internal and external

Fig. 1. (a) 5th rib of S605 and coupon design, (b) μCT-scan reconstruction, (c) Representation of cortical bone thickness for sample location.

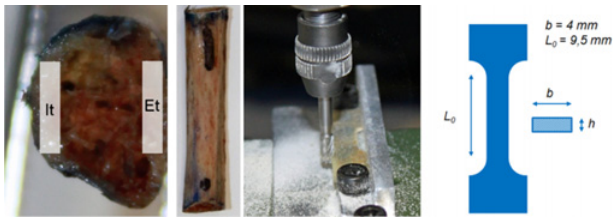

Fig. 2. (a) Illustration of the rib section and localisation of cortical bone sample (Et: External table and It: Internal table), (b) flat coupon coupons, (c) machining of bone sample, (d) dimensions of the bone coupons.

tables (figure 1(a)) are completely dissociated. As the two extremity parts of the sample will be fixed into wedge grips, the parallelism should be focused on the calibrated zone of the sample length. The second step consists to remove the trabecular bone in order to have a cortical bone sample, with a representative thickness. The trabecular bone removal is operated gradually with a STRUERS TegraPol-11 polisher, equipped with fine polish grain at 400.

Last step is to machine the flat bone sample using a μ milling machine (PROXXON MF70 with a drill diameter of 3 mm). This machine guarantees the shape control and parallelism condition on the calibrated zone, where the sample will be subject to tension. At the end of this preparation protocol, the calibrated zone has parallel edges, as recommended for tensile tests, but the prismatic shape of the sample is not perfect. This flatness is crucial to estimate the real resisting section area, and to compute the true stress of the sample. For each sample, the apparent density (ϱ_{app}) was also calculated according to the Archimedes' principle. This measurement consists in the comparison of the specimens' weights in air and in water. In order to have the real geometry of each sample, 2 kinds of measurements are considered: Classical one and measurements coming from μCT data.

Sample measurements (figure 2(d)) are taking with electronic digital calliper: thickness (h), calibrated zone length (L_0) and width (b). μCT data gives information of these same parameters with higher precision. Because of the thin thickness of sample, a μCT-scan device was the best application to measure precisely the section bone area (B_a), which corresponds to the real cross section. Finally, the real shape of sample is determined and associated with the porosity in each section. The aim of this measurement is to calculate correctly the stress value with the current section (S_0).

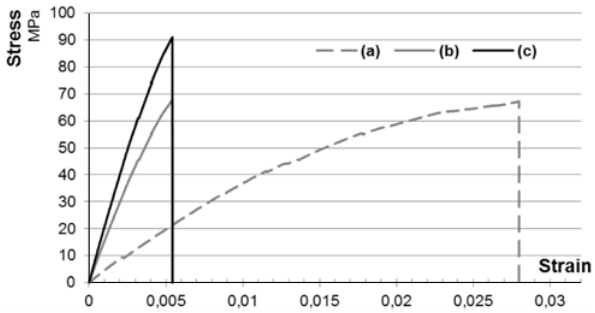

Fig. 3. Computing method, explanation about correction – (a) Without strain gage and Classical cross section measurement, (b) With strain gage and Classical cross section measurement, (c) With strain gage and μCT cross section measurement.

2.2 Mechanical test

The 14 samples coming from the 2nd to 10th rib of the PMHS was instrumented with strain gages. This gage is glued in the centre of each sample using cyanoacrylate adhesive. The gage grid line was oriented in the tension direction. For a better electrical noise level, the gages are coupled to a Wheatstone bridge circuit. The nominal resistance of gage is 350 Ohms at 2 V and the net grid length is 1.57 mm. The strain sensitivity is ±3%. As this study is focused on tensile test on thin cortical bone, an adapted machine (Instron ElectroPuls Dynamic E3000) was used with adapted wedge grips and suitable force cell (DYNACELL 3kN). All the tensile tests are performed at a constant loading velocity of 1 mm/min. The analysis performed in the present study takes into account that material is homogenous and isotropic. Consider those hypotheses, the strain-stress results are discussed in term of engineering stress (axial force divided by the resisting initial cross-section area) against the engineering strain (displacement divided by the initial length of the calibrated zone).

The figure 3 illustrates the different corrections applied on the result of a single sample. The curve A is obtained with classical cross section measurement S_0 and the displacement given by the tension test machine (without strain gage measurement). The sample area S_0 is calculated by an electronic digital calliper. In order to overcome the sliding in the wedge grips, the curve B referred to the same cross section measurement but a correction is made with the true strain coming from the gage signal. Last curve (C) introduces another significant correction with the section bone area S_0 using the μCT data value. As mention previously, this area is overestimated when a classical method is used. In this third case, the mean section on the useful length is employed.

As a conclusion of this comparison, the mechanical behaviour is analysed in term of true strain (strain gage signal) and engineering stress using the initial section bone area from μCT-scan data. Mechanical tests results were analysed in the frame of THOMO project and revealed a different mechanical behaviour of cortical bone and Internal and External table.

The analysis also included also other ribs parameters such as the location of the sample in rib (Rib number, rib

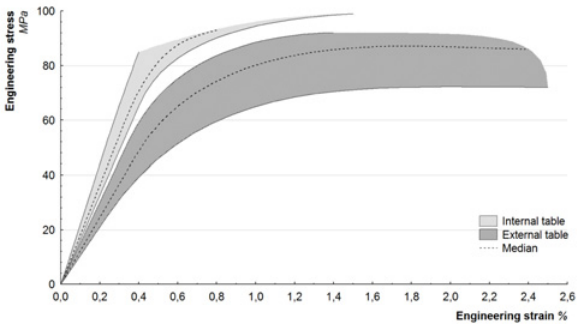

Fig. 4. Mechanical behaviour obtained on quasi-static for cortical bone (external and internal tables of rib).

length position, internal and external tables) and density measurement. An important difference of the strain at failure is observed between the internal (median value at 0.75%) and external table (2.41%). The location difference is quite similar concerning the stress at failure but dispersion is more important on external table. In order to establish a mechanical law, a strain/stress corridor is plotted on figure 4 from the 14 samples (8 samples harvested on external table and 6 on internal one). A corridor (figure 4) was established in order to represents the mechanical law of the cortical bone thickness of one subject.

2.3 Design of Hopkinson bars

The access to higher rates of strains, Hopkinson bars technique are classically required whatever compression or tension loadings. Classical designs of measurement bars are not suitable for this purpose due to the complexity of specimen's geometry (thickness variation). The main difficulty is due to the behaviour of the coupon itself, in particular the cross section is not homogeneous and very small (few mm^2). Therefore, the calculation of the strain-stress curve cannot be determined accurately; in fact the amplitude of the transmitted is very limited and the amplitude of the reflected is close to the incident pulse so that the output force is noisy. In this context, a new design of SHTB is studied here on the basis on a Finite Element approach of the set measurement bars/biological coupon. For this revision of the Kolsky [9] technique, the identified mechanical behaviour on quasi-static loading (figure 4) is used as input data for FE aided design of dynamic device.

Finite Element simulations have been conducted using Abaqus explicit code by varying the design configuration, mainly for the diameter and the constitutive material of the bars. The Finite Element model is composed by 75000 solid elements for each bar. The sample is modelled using the geometrical analysis of the coupon tested under quasi-static conditions and finally composed by 2400 solid elements (figure 5). All experimental testing conditions have been respected and the forces' equilibrium has been systematically checked. As the coupon is loaded in tension, the striker is tubular and accelerated once a velocity of $9\,m.s^{-1}$ is reached before the impact with the input bar. The measurement of the elastic waves propagating along the input bar is taken at the mid-length of the incident bar. The

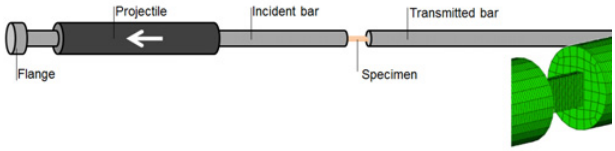

Fig. 5. Schematic and FE model of the Split Hopkinson tensile bars set-up.

measurement of the transmitted elastic wave is obtained at 100 mm from the coupon.

The first step of the design approach consists in the determination of the length of the tubular striker assuming that the same material is used for the bars. As the strain at fracture ε of the cortical structure is quantified close to 3%, the duration time τ is calculated once the lowest strain rate is defined (equation (1)). Here, a strain rate fixed to an average value of $200\,s^{-1}$ conduces to a duration time of the elastic wave propagating along the input bar equal to $150\,\mu s$. Equation (2) converts the time space to dimensional space, thus the length L of the striker. As the speed wave C is given for the constitutive material of the striker, the length of the striker is determined and the length of the input bar is at least multiplied by 2.

$$\varepsilon = \dot{\varepsilon}.\tau \tag{1}$$

$$\tau = 2.\frac{L}{C} \tag{2}$$

As the striker has a tubular shape, it must have an equivalent diameter in accordance with mechanical impedance relations recalled in equation (3):

$$\rho_{\text{striker}} \times C_{\text{striker}} \times S_{eq} = \rho_{IB} \times C_{IB} \times S_{IB} \tag{3}$$

Concerning the tested sample, the material behaviour of the cortical structure of the human rib is considered prior to the optimisation of the bars' design. As explained previously, the stress at failure is quite similar for both internal and external tables but the maximum strain follows 2 tendencies. The study is based on the cortical sample coming from external table whereas the median value of strain is more important than internal table.

The material arrangements of the device are given as following:

+ input bar/output bar: Al6060 ($5 < Ø < 25$ mm),
+ input bar/output bar: Pa66 ($10 < Ø < 25$ mm),
+ input bar: Al6060, output bar: Pa66($12 < Ø < 25$ mm).

3 Results

As mentioned in section 2.4, the optimal configuration is obtained once the amplitude of the output wave is well balanced regarding the amplitude of the incident wave. In this context, the projectile length is computed in function of the material properties of wished bars, the strain and strain rate of sample. As explained previously, the optimisation is associated to the rib's cortical bone properties. The choice was fixed on the external table because of the tested samples presented a more important strain (2.41%)

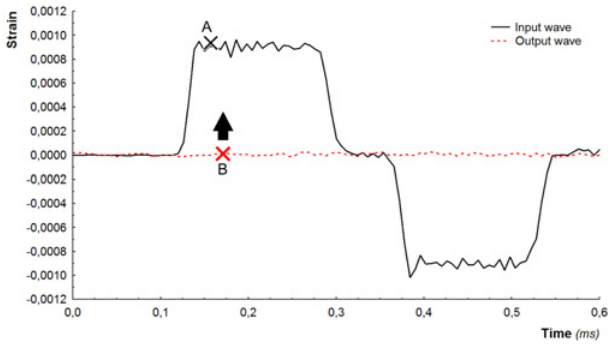

Fig. 6. Input and output waves' signals on aluminium bars (Ø25 mm).

in this anatomical part. The model is constructed thanks to this strain augmented at 3% to guaranty the mechanical response in the duration time of the incident pulse. The first configuration is composed of cylindrical bars made of Al 6060 alloy. The cylindrical bars have a young modulus equal to 70 GPa and a density fixed to 2700 kg.m^{-3}. The wave's speed of the aluminium is about 5014 m.s^{-1}. Projectile and bars lengths are computed for aluminium configuration in function of equations (1) and (2). Finally, the length of the tubular striker is equal to 400 mm. The length of the input and output bars are extended to 1.2 m so as to avoid any reflection of the elastic waves' system. All calculations as performed with a Matlab© routine that generates automatically a FE model with adaptive mesh size. This model is expanding to 10 models where diameter of the bar can be adjusted.

In order to highlight the input (A – figure 6) and output signals used for the governing equations (Kolsky [9]), the elastic strain are plotted in function of time in figure 6. Aluminium bars with 25 mm in diameter are modelled to illustrate the technological restrictions. In that dramatically configuration, the amplitude of the output bar is quite negligible (B – figure 6), so that any further calculations can be performed in the elastic wave's analysis. As the goal of optimisation design is based on the elastic deformation of the output bar, the solution consists to reduce significantly the diameter of the measurement bars as mentioned by Zhao [9] on the basis of mechanical impedance balance. In that approach, a natural amplification of the elastic pulse is proposed prior to electrical amplification where noise level is coupled.

The FE modelling programme consists to evaluate a set of 10 configurations where the diameter varies from 5 to 25 mm for each bar (input/output 5 to 25 in figure 7). The transmitted pulse with the highest amplitude is ensured using a cylindrical bar with a 5 mm in diameter. Configurations between 10 and 25 mm revealed a low-level response (less than 10% regarding the amplitude of the input signal). Here is confirmed that SHTB with small diameter is one solution to test accurately biological segments with low mechanical properties.

For the considered tensile tests, the amplitude of the elastic wave generated in the output bar is naturally amplified using bars with a small diameter but as a consequence, technical difficulties appear. For instance, gripping system and alignment control reveals very challenging.

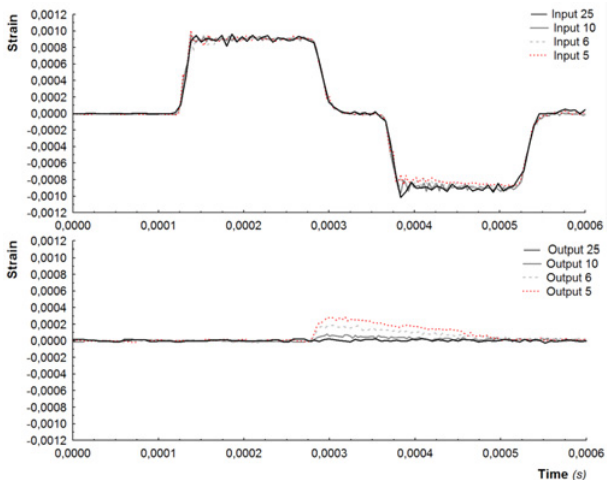

Fig. 7. Typical signals on aluminium bars, a- Input signal, b- Output signal.

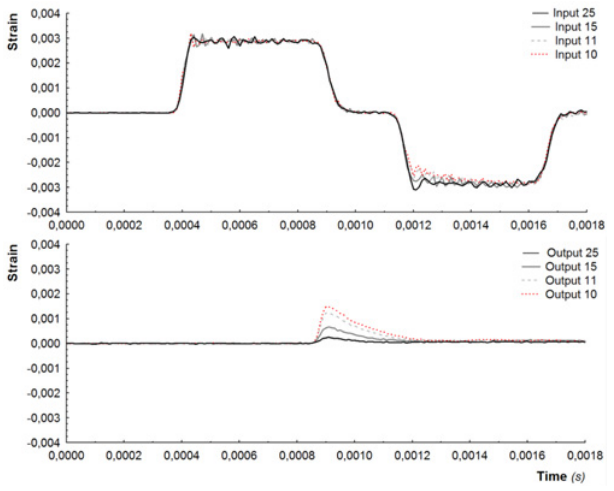

Fig. 8. Typical signals on nylon configuration, a- Input signal, b- Output signal.

Here, a modification of the constitutive material of the bars is proposed to increase once again the natural amplification of the transmitted pulse. The same Matlab© routine is employed with cylindrical bars made of Polyamide 66 (E = 3 GPa, mass density = 1150 kg.m^{-3}). The wave's speed in nylon is about 1800 m.s^{-1} so that the length of the projectile can be reduced with a ratio close to 3, thus 150 mm in length with respect to the attended strains at break. The length of bars in this configuration is limited to 500 mm. Numerical simulations are performed with respect to the same loading conditions previously detailed. F.E. models were declined between 10 and 25 mm in diameter for each bar. The typical input and output signals produced after the impact with the striker are plotted on figure 8.

Here, F.E. simulation confirms that an output bar with 15 mm in diameter is efficient to capture precisely the current force during the tension of the coupon. Moreover, the diameter is large enough to design special gripping systems to hold both side of the coupon.

A final configuration is proposed for an input bar and a projectile composed of aluminium and the output bar is

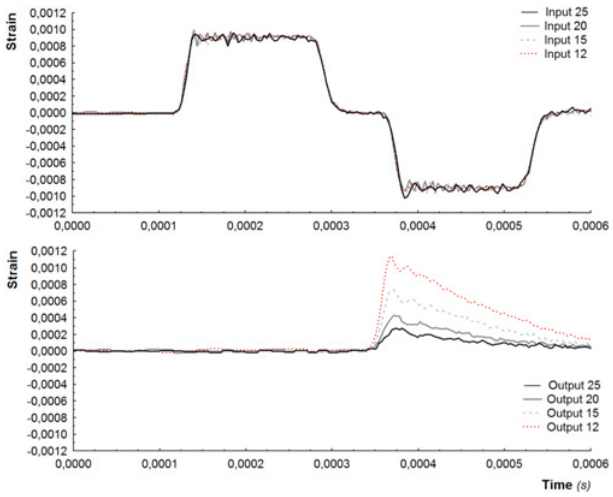

Fig. 9. Typical signals, a- Input signal (aluminium bar), b- Output signal (Pa66 bar).

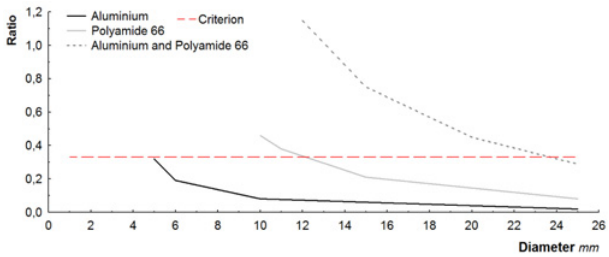

Fig. 10. Input vs. Output elastic waves amplitude with respect to the diameter of the set-up.

made on Pa66. Dimensions of the set-up are based on the first configuration were the constitutive material of the projectile and the incident bar was aluminium. The different detected signals on 4 configurations are given in figure 9. The velocity of the striker before the impact is kept equal to 9 m.s^{-1}. The main interest of this configuration is to ensure high rate of loading got by striker/input bar without any damage of the loading system.

Finally, the results of the different configurations are summarized in figure 10. The dotted red line represents the following relation (4):

$$r = \frac{\varepsilon_{TRA}(t)}{\varepsilon_{INC}(t)} \tag{4}$$

where r is the ratio between the mean transmitted pulse amplitude and the mean incident pulse amplitude. A ratio over 0.33 is generally recommended to ensure an acceptable separation of the incident wave between its reflected and transmitted part propagating through the coupon. Here are then removed the undesirable solutions, thus below the dotted line in red.

A reasonable configuration for the set-up developed for further tensile tests on coupons extracted from humans' ribs can be detailed hereafter. The cylindrical bars should have a diameter close to 10 mm and are made of Polyamide 66.

In figure 11 is illustrated the check of the equilibrium of the input and output forces near the biological coupon. It is clearly demonstrated that this statement cannot be

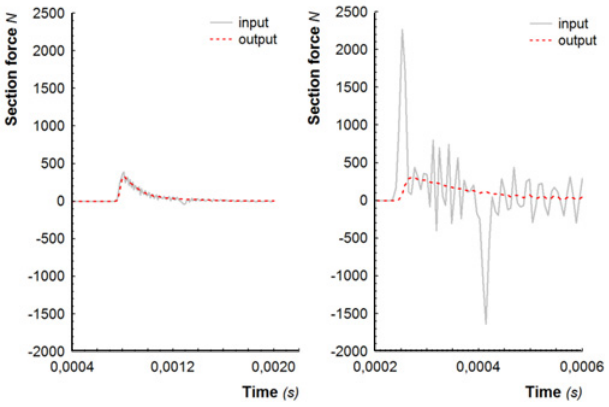

Fig. 11. Forces' equilibrium, a- Pa66 cylindrical bars Ø12 mm, b- Al6060 and Pa66 cylindrical bars Ø20 mm.

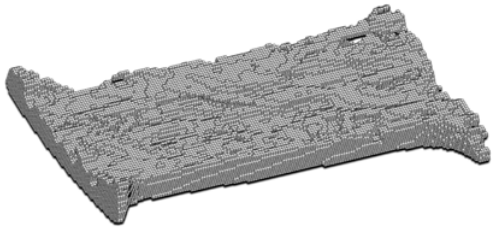

Fig. 12. F.E model of a flat coupon extracted from a human's rib.

obtained on the basis of Aluminium bars because the reflected wave is very noisy and not give the opportunity to calculate precisely input force, strain, strain rate in function of time. On contrary, the forces-time curve given in 12-a show that the reflected pulse is representative so that the input force is accurately calculated in accordance with the output force (equations (5) and (6)).

$$F_{IN}(t) = S_{IN}.E_{IN}(\varepsilon_{INC}(t) + \varepsilon_{REF}(t)) \tag{5}$$

$$F_{OUT}(t) = S_{OUT}.E_{OUT}.\varepsilon_{TRA}(t) \tag{6}$$

4 Discussion and conclusions

This study revealed a main interest on the preparation of flat coupons of biological tissues. Mechanical test on biological material success is conditioned by an optimal sampling procedure. Harvesting cortical samples from fresh ribs dedicated to tensile tests is a challenging task due to the geometry (figure 1). As the human ribs have thin cortical bone thickness, it was interesting to combine the sample preparation to the geometrical measurement with high precision level. This accurate analysis is performed thanks to a μCT scan device and gives the opportunity to capture the real shape of cortical coupon associated with the location of each sample on the thorax.

These μCT measurements are added on the experimental test analysis, numerical design of SHTB and FE model development (figure 12). The real shape of bone coupon could be used on numerical simulation in order to evaluate more precisely the mechanical behaviour during testing sequence. The present study under quasi-static

loadings revealed different mechanical responses between internal and external tables. As the geometry of biological tissues is definitively attained at a microscopic scale, it is challenging to keep a similar precision in the loading process of the coupon both under quasi-static and dynamic conditions. For that, cylindrical bars with small diameter are proposed for tests performed under dynamic conditions so as to check if the mechanical trends defined previously are confirmed. But, these statements are achieved on condition that measurement bars are sensitive in accordance with the mechanical properties of the considered specimens. A sensitivity study based on the influence of both material and geometrical properties of the cylindrical bars on the amplitude of the elastic waves' system propagating along the bars is lead. In a near future, Nylon tensile bars with 12 mm diameter will be equipped and calibrated to perform tensile tests on coupons extracted from human ribcage. Special attention will be given to the holding system to ensure any influence on the mechanical response during the test.

Acknowledgements

The present research work is also supported by the International Campus on Safety and Intermodality in Transportation (CISIT), the Nord-Pas-de-Calais Region, the Regional Delegation for Research and Technology, the Department of Higher Education and Research, and the National Centre for Scientific Research (CNRS). The authors gratefully acknowledge the support of these institutions. This work could not have been done without the generous gift of body donors, through the body donation program of the University of Paris. A special thought to all of them.

References

1. Kuppa S., Eppinger R., 42nd *Stapp car crash conference proceedings*, 139-154 (1998).
2. Vezin P., Berthet F., *Stapp car crash journal,* **53**, 93-125 (2009).
3. Robin S., *Proce.edings of the 17th international technical conference on the enhanced safety vehicle*, 297 (2001).
4. Song E., Trosseille X., Baudrit P., *Stapp car crash journal,* **53**, 155–91 (2009).
5. Ferreira F., Vaz M., Simoes J., *Materials Characterization*, **57**, 71–79 (2006).
6. Wright T.M., Hayes W.C., *Medical and biological engineering*, **14**, 671-681 (1976).
7. Subit D., del Pozo de Dios E., Valazquez-Ameijide J., Arregui-Dalmases C., Crandall J., arXiv: 1108.0390 (2011).
8. Kemper A.R., McNally C., Kennedy E.A., Manoogian S.J., Rath A.L., Ng T.P., Stitzel J.D., Smith E.P., Duma S.M., Matsuoka F., *Stapp Car Crash Journal*, **49**, 199–230 (2005).
9. Kolsky H., *Stress waves in solids*, 211pp25s (1953).
10. Zhao H., *Thesis,* (1992).